Numerical characterization of optical properties of tapered plasmonic structure on a cantilever pyramidal tip for plasmon nanofocusing

Cite as: AIP Advances 12, 085216 (2022); doi: 10.1063/5.0106066
Submitted: 27 June 2022 • Accepted: 29 July 2022 •
Published Online: 24 August 2022

Ravi Yadav,[1] Takayuki Umakoshi,[1,2,3] and Prabhat Verma[1,a)]

AFFILIATIONS

[1] Department of Applied Physics, Osaka University, Suita, Osaka 565-0871, Japan
[2] Institute for Advanced Co-Creation Studies, Osaka University, Suita, Osaka 565-0871, Japan
[3] PRESTO, Japan Science and Technology Agency, Kawaguchi, Saitama 332-0012, Japan

[a)] **Author to whom correspondence should be addressed:** verma@ap.eng.osaka-u.ac.jp

ABSTRACT

The plasmon nanofocusing process has been widely implemented in near-field scanning optical microscopy (NSOM) recently because it allows generating a background-free nanolight source at the apex of a metallic tip, enabling high contrast imaging at the nanoscale. In plasmon nanofocusing-assisted NSOM, the metallic tip properties play a vital role in generating an intense and well-confined nanolight source by controlling the plasmons' behavior. This is why various tip designs have been developed so far. Recently, our group has also developed a metallic tapered tip, composed of a dielectric pyramidal base and a thin metallic layer coated on one side of the pyramid, using a novel fabrication method that allows tuning the optical properties of a tip depending on the requirement. Although our metallic tip has a unique advantage of tuning its optical properties, it has not yet been well studied. In this work, we present a thorough study of the optical properties of our metallic tip that depends on its parameters, such as the dielectric material, metal thickness, and cone angle, using finite-difference time-domain simulations. This particular study will allow us to understand controlling the tip's optical properties and expand it for a wide range of applications.

I. INTRODUCTION

Optical antennas have played a central role for decades in the field of nanophotonics to control light at nanoscale. A gold nanorod, for instance, generates intense nanoscale light sources at both its ends through localized plasmon resonance when illuminated with visible light. Such a strong nanolight source has produced a variety of nanophotonics applications.[1–8]

Apart from localized plasmon resonance, plasmon nanofocusing is a phenomenon that has been recently recognized as an alternative way to create a nanolight source.[9–12] In plasmon nanofocusing, a metallic tapered structure with a nanometrically sharp apex is employed. In this process, plasmons are usually excited at a plasmon coupler, e.g., a grating structure, located on a shaft of the metallic taper at a reasonably large distance from the apex. The excited plasmons then propagate on the tapered structure toward the apex by compressing their energies and eventually create a strong nanolight source at the apex. Because the plasmon coupler located on the shaft is far from the apex, one of the strong advantages of this technique is that the nanolight source created at the apex is spatially separated from the incident light. This excludes the possibility of direct illumination of the sample with incident light, effectively eliminating any possible background scattering and other noises generated by the incident light. Plasmon nanofocusing thus holds great potential for various nanophotonics applications.[13–16] One of the great candidates to examine plasmon nanofocusing is near-field scanning optical microscopy (NSOM).[17] Since a similar metallic needle is utilized in conventional scattering type NSOM, one can immediately adopt plasmon nanofocusing for NSOM. It allows us to create near-field light at the tip apex without any interference from the incident light, leading to high image contrast. Several previous reports have already shown the great benefits of plasmon nanofocusing for near-field optical imaging.[17,18]

For plasmon nanofocusing-assisted NSOM, the metallic tapered tip plays a crucial role to excite effective plasmon nanofocusing and create strong near-field light at the apex. A metallic conical tip is one of the most common tip structures used for nanofocusing because one can easily fabricate it by the electrochemical etching method.[12,13] Besides, a conical tip made by electrochemical etching can be easily attached to a tuning fork that has been widely used in NSOM apparatuses for precise control of the tip position. However, a drawback is that since chemical processes are involved in fabrication of the tip, the plasmonic material used is mostly limited to gold, which thus limits the wavelength range to around the near-infrared region. This is because in the case of silver and aluminum, which are suitable plasmonic materials for the visible or ultraviolet region, fabricated structures become rough through the chemical etching reaction, which hinders plasmon propagation and efficient plasmon nanofocusing. Only in the case of gold, reliable conical tips with smooth surfaces have been obtained under optimized fabrication conditions.

We have recently developed a novel fabrication method of metallic tapered tips for plasmon nanofocusing-assisted NSOM. We used a commercially available silicon cantilever that has a pyramidal tip at the end. By depositing a metallic film through vacuum evaporation on one surface of the pyramid as a base structure, a two-dimensional tapered structure was easily and automatically formed. Furthermore, by keeping the evaporation direction perpendicular to the tip surface and making the evaporation rate faster, an atomically smooth tapered coating was obtained. Since this method is based on physical vapor deposition, one can basically choose any metal, including typical plasmonic materials such as gold, silver, aluminum, copper, and so on. In fact, we have fabricated a tapered structure made of silver on a cantilever tip, on which a plasmon coupler was fabricated in the form of a grating structure by means of focused ion beam (FIB) lithography. Since the entire tip is fabricated on a cantilever, there is no need to attach the tip, for example, to a tuning fork, and hence, it can be immediately applied as it is for NSOM measurements, which we have successfully demonstrated previously through near-field optical imaging of carbon nanotubes.[17] Moreover, as the smooth coating facilitates efficient plasmon propagation with low energy loss, plasmon nanofocusing was highly reliable and reproducible. In addition, we recently confirmed that this method works for gold, silver, and aluminum, and plasmon nanofocusing was excited for the entire whole visible range.[19] Despite the strong potential of this novel tip design for plasmon nanofocusing-assisted NSOM, fundamental optical properties, such as intensity and the spatial extent of near-field light, have not yet been extensively investigated, and their dependence on structural parameters of the tapered tip design, e.g., base material, cone angle, and coating thickness, remains uninvestigated.

In this study, we show numerical investigations of pyramidal-tip-based tapered structures to understand the fundamental optical properties for plasmon nanofocusing. We evaluated the structural parameters of the tip to characterize optical properties such as intensity and the spatial extent of near-field light at the tip apex. For example, for atomic force microscopy (AFM) cantilever tips, several types of cantilever materials are available, which serve as the base material for tips and affect the plasmon nanofocusing process. The thickness of a tapered metallic layer coated on the tip should also modify the optical properties of tips. The cone angle is another important factor as well. As these are representative structural parameters for our tapered tip design, we have quantitatively examined how effective these parameters are for the plasmon nanofocusing process. This study would give fundamental and practical insight to understand the optical properties of this unique tip design that will help in extending it further to near-field optical applications based on plasmon nanofocusing in a much efficient way.

II. RESULTS AND DISCUSSIONS

Figure 1(a) shows a simulation model for the tip design used in this study. We utilized the finite difference time domain (FDTD) method (Poynting for Optics, Fujitsu) for electromagnetic simulation of our model during plasmon nanofocusing. We designed a pyramidal tip with an apex that has a diameter of 20 nm. The material of the pyramidal tip can be changed by setting the permittivity to that of silicon, silicon nitride, and so on. A silver layer was coated on one surface of the pyramidal tip, the thickness of which was adjusted for each simulation. The cone angle was also varied to investigate its dependence. A grating structure was designed on the silver layer, which is located 4 μm away from the apex. In this study, we adopted an incident wavelength of 642 nm as the typical wavelength used in various optical measurements, and thus, silver was chosen as the plasmonic material, which gives the best optical property for this particular wavelength. We set the refractive index and extinction coefficient for silver as 0.5 and 4.34, respectively.[20] The real and the imaginary parts of permittivity for silver were taken as -18.89 and 0.47, respectively.[20] The incident light has an electric field profile of a Gaussian shape that is assumed to focus at the grating with a numerical aperture of 0.2 and with a beam diameter of around 1900 nm. We used a non-uniform mesh in our simulations to save calculation time for such a large calculation model of several micrometer scales. The mesh size around the tip apex was 2 nm, while it was set to 5 nm around the grating structure. The mesh size in other regions was 20 nm. Perfectly matched layers were employed as the boundary condition at around the simulation model, which absorbs light moving out from the calculation region to get rid of reflection artifacts. A point detector was located 6 nm below the tip apex to monitor the near-field light intensity, the distance of which is far enough to avoid artifacts due to discretization of the calculation model.

We first investigated the dependence on the base material of the cantilever tip. For the material of AFM cantilevers, the most common ones are silicon and silicon nitride. In addition, one can easily obtain oxidized silicon cantilevers by oxidizing silicon cantilevers in an electric furnace with water vapor, as demonstrated previously.[2,7,17,18] We therefore chose these three materials to investigate their influence on plasmon nanofocusing. For silicon, we set the refractive index and extinction coefficient to 4.19 and 0.39, where the real and the imaginary parts of permittivity were 17.40 and 3.31, respectively.[21] The refractive index and the extinction coefficient of silicon nitride were set to 2.01 and 0.0, respectively. Accordingly, the real and the imaginary parts of permittivity for silicon nitride were 4.08 and 0.0, respectively.[22] For oxidized silicon, the refractive index, extinction coefficient, and the real part and the imaginary part of

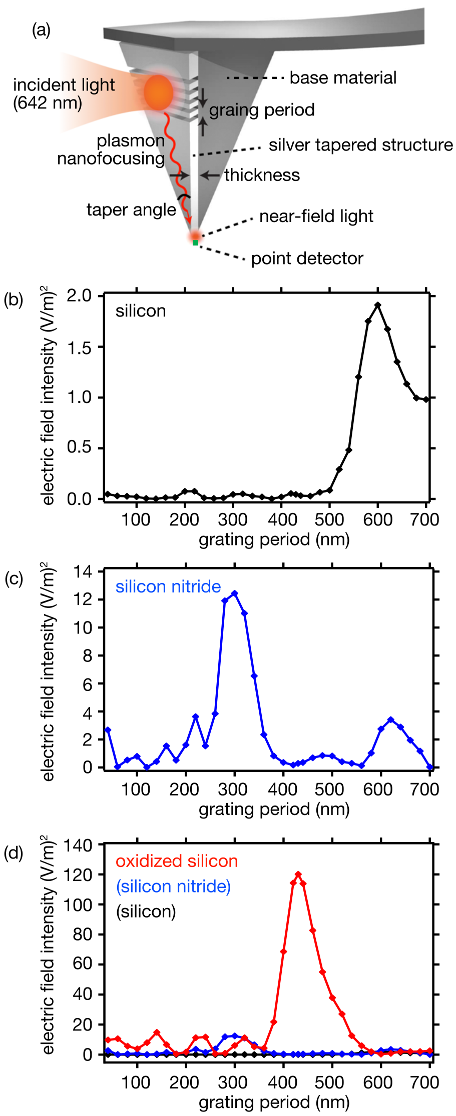

FIG. 1. (a) FDTD simulation model used for plasmon nanofocusing. Relationship between near-field light intensity at the tip apex and the grating period (b) in the case of silicon used as a base material, (c) in the case of silicon nitride as a base material, and (d) in the case of oxidized silicon as a base material. The curves shown in (b) and (c) are overlayed in (d) at the same scale of electric field intensity for comparison.

permittivity were 1.46, 0.0, 2.12, and 0.0, respectively.[23] In this simulation, the thickness and cone angle were fixed to 40 nm and 28°, respectively, referring the previous work.[17,18]

We then compared near-field light intensity obtained at the tip apex between these materials. Because the base material modifies the plasmonic properties of silver tapered structure, the grating period for the best plasmon coupling should be different between materials to maximize the coupling efficiency. To fairly compare between these materials, we started by evaluating the best grating period for each material. As shown in Figs. 1(b)–1(d), each material showed the best coupling peak at different grating periods. In the case of silicon, the highest near-field light intensity was obtained at a grating period of 600 nm. For silicon nitride, the best grating period was 300 nm, whereas it was 420 nm for oxidized silicon. During the process of nanofocusing, surface plasmons propagate on both interfaces, namely, the silver/air and the silver/base material interfaces. With proper selection of the silver thickness, the two propagating plasmons do not interact with each other, and hence, one can observe peaks corresponding to both propagations independently. Our simulation reveals that the peak observed at about 600 nm corresponds to the plasmon propagation at the silver/air interface, which can be distinctly observed for silicon and silicon nitride; however, it is not very clearly seen for oxidized silicon due to its weaker strength. Our simulation also confirms that plasmons propagating at the interfaces of silver/silicon, silver/silicon nitride, and silver/oxidized silicon correspond to peaks at 43, 283, and 415 nm, respectively. Since 43 nm is too far from the incident wavelength of 642 nm, there is no photon–plasmon coupling due to a large wave vector mismatch, and hence, Fig. 1(b) shows only one peak corresponding to the plasmon propagation at the silver/air interface. On the other hand, one can achieve a wave vector match at 283 nm for the silver/silicon nitride interface and at 415 nm for the silver/oxidized silicon interface by tweaking the grating period, which correspond to the peaks observed at around 300 and 420 nm, respectively, shown in Figs. 1(c) and 1(d). We, at the same time, found that the coupling efficiency and the resulting near-field intensity were drastically decreased to almost 0 if the grating period was not properly designed, which emphasizes how important it is to optimize the grating period for plasmon nanofocusing.

We also found that the base material significantly affected the near-field light intensity. Note that the intensity scales shown in Figs. 1(b)–1(d) are not the same. For comparison, the curves of grating period dependence shown in Figs. 1(b) and 1(c) are also overlaid in Fig. 1(d) in the same scale of the near-field intensity. At the optimized grating period, the near-field intensity was only about 1.9 $(V/m)^2$ in the case of silicon, which increased to 12.4 $(V/m)^2$ for silicon nitride. On the other hand, we obtained a near-field intensity of 120.0 $(V/m)^2$ in the case of oxidized silicon. Therefore, the oxidized silicon tip provided around 10 times stronger near-field intensity than the silicon nitride tip and 63 times stronger near-field intensity than the silicon tip. We guess that such a huge difference between silicon and oxidized silicon is mostly due to the extinction coefficient. As mentioned above, silicon possesses the large extinction coefficient, which could lead to large energy dissipation resulting in weak near-field intensity at the tip apex. On the other hand, in the case of oxidized silicon, its extinction coefficient is 0 as it can be regarded as a transparent glass, which facilitates efficient plasmon nanofocusing. In this sense, the extinction coefficient is 0 for both oxidized silicon and silicon nitride; however, the near-field intensities are quite different. This can be due to the larger refractive index or the larger real part of permittivity for silicon nitride. The larger refractive index indicates a longer optical path length for plasmons to propagate from the grating structure to the tip apex. Even though the extinction coefficient is 0 in the base material, silver itself has the high extinction coefficient of 4.34. Therefore, plasmons could be dissipated faster during its propagation for a longer optical length in the case of silicon nitride compared with oxidized silicon. Since much of the plasmon nanofocusing process is governed by propagation of plasmons, such differences in optical properties of base materials resulted in a huge variation in the obtained near-field light intensity. These results clearly indicate that at least a silicon nitride cantilever should be utilized rather than silicon cantilevers for plasmon nanofocusing. However, if an electric furnace or any other machines are available for oxidation, oxidizing a silicon cantilever tip is the best solution to obtain a strong near-field light as it gives 10 times stronger near-field intensity than with the case of silicon nitride. Unfortunately, to the best of our knowledge, an oxidized silicon tip is not commercially available yet, or at least it is not a very common product. Therefore, we suspect that some facility for oxidation is required to employ oxidized silicon cantilever tips for plasmon nanofocusing. Here, one should note that each type of cantilever has different physical properties, and thus, the results do not simply mean that cantilevers other than oxidized silicon cantilevers are useless. For example, it is known that silicon nitride cantilevers are very soft, i.e., they have low spring constants compared with silicon cantilevers or oxidized silicon cantilevers, as they are usually used as bio-cantilevers. Therefore, in the case where one observes bio samples or any other fragile samples, a silicon nitride cantilever might be employed at the cost of the plasmon nanofocusing efficiency and the resulting near-field intensity.

Furthermore, we evaluated the spatial volume of near-field light created at the tip apexes between different base materials by choosing grating periods that best suited each material. Figure 2(a) shows the calculated electric field distributions at around the tip apexes for different materials of cantilever tips. We clearly observed huge differences in near-field light intensities in these electric field distribution images as well. To analyze the spatial extent of near-field light, we took line profiles of near-field light intensities along with the white dashed lines indicated in Fig. 2(a), which are shown in Fig. 2(b). All the line profiles showed Gaussian distribution of near-field light intensities. In the cases of silicon nitride and oxidized silicon, we observed an almost same line profile, where the full width at half maximum (FWHM) of the peak was around 33 nm. Interestingly, on the other hand, we observed a sharper peak for the silicon cantilever tip. The FWHM was around 24 nm, which is 1.37 times narrower than in the cases of silicon nitride and oxidized silicon. This indicates strong confinement of near-field light, which directly contributes to better spatial resolution in near-field measurements than other materials. We guess that the much higher refractive index of silicon is attributed to this strong confinement. The silicon tip apex sits next to the apex of the silver tapered structure and would affect the spatial extent of the near-field light. Therefore, strongly confined near-field light could be obtained due to the high refractive index of 4.18, which shrinks the mode volume of the propagating plasmon, although it also causes higher propagation energy loss. Therefore, with respect to the near-field light intensity, a silicon cantilever tip is not appropriate to be used for plasmon nanofocusing. However, there could be a possibility to employ the silicon tip for plasmon nanofocusing in case a higher spatial resolution is required. For example, the silicon cantilever tip can be a right choice for some samples that are optically active and does not require strong near-field light illumination to emit optical signals strong enough to be detected. Although the process of plasmon nanofocusing itself is not efficient, one can easily perform near-field measurements at better spatial resolution with a silicon cantilever tip.

Overall, we found that base materials have a strong impact on the plasmon nanofocusing process in our particular tip design. In terms of near-field light intensity, oxidized silicon is much better as a base material than silicon nitride and silicon; however, oxidation facility is necessary. At this point, silicon nitride cantilever

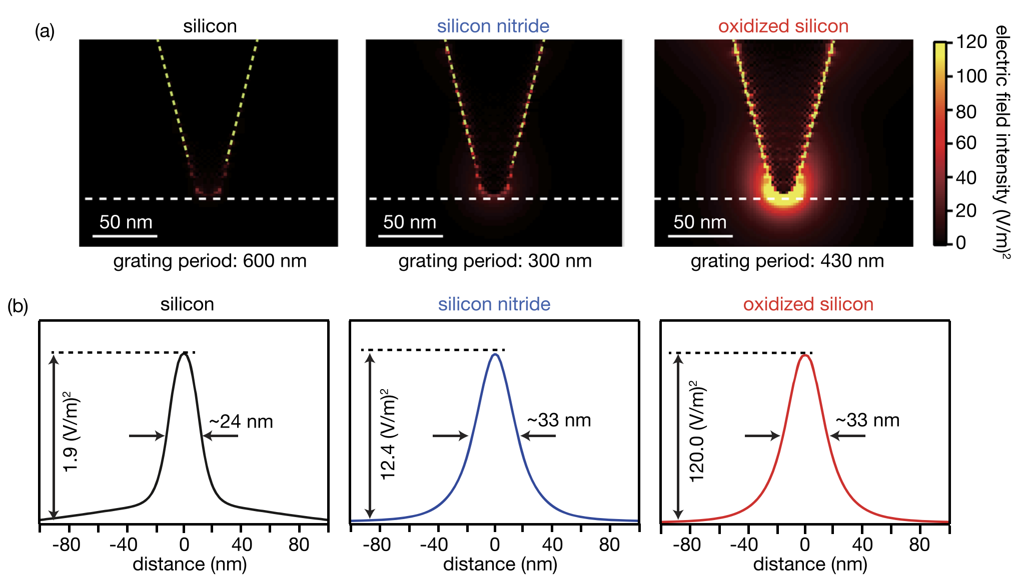

FIG. 2. (a) Distribution maps of electric field intensities for the cases of silicon, silicon nitride and oxidized silicon tips as base materials. (b) Line-profiles of electric field intensities obtained at white dashed lines in (a) for each base material.

tips are commercially available, and moderate intensity of near-field light can be still obtained. Moreover, the softness of the silicon nitride cantilever tips is beneficial for soft, fragile samples such as bio-molecules. Compared with oxidized silicon and silicon nitride, silicon showed much less efficiency of plasmon nanofocusing; however, it can still be useful in the case where spatial resolution is of importance in near-field measurements. It can shrink the spatial volume of near-field light so that one can easily obtain better spatial resolution. Since the near-field light intensity for silicon is much weaker than that for other materials, the use of silicon cantilever tips would be limited for bright samples that do not require strong near-field light for optical measurements.

Next, we investigated the effect of thickness of the silver tapered structure, which is an important parameter that should be controlled in actual experiments by adjusting the conditions of vacuum evaporation for silver coating. Here, we fixed a base material to oxidized silicon, considering its capability of efficient plasmon nanofocusing. The cone angle was taken as 28°, which is one of the values of the cone angle for commercially available cantilever tips, and the grating period was set to the optimum value of 430 nm, as estimated in Fig. 1(d). We changed the silver thickness from 10 to 120 nm. Figure 3 shows the dependence of near-field intensity on the coating thickness. Interestingly, we observed a peak at a thickness of 50 nm, which showed the strongest intensity of 142.0 $(V/m)^2$. As the thickness increased from 50 nm, the near-field intensity gradually decreased. Similarly, by decreasing the thickness from 50 nm, the intensity decreased and dropped down to almost 0 for thicknesses smaller than 20 nm. The reason for the intensity decrease for thickness layers less than 50 nm can be understood from the weaker near-field light and confinement of near-field light at the apex. The tip apex size becomes large as the thickness increases, leading to a weaker confinement as well as lower optical intensity of near-field light. However, this effect should enhance the near-field intensity for thicknesses smaller than 50 nm, which is opposite to the calculation results. At a thickness of less than 50 nm, we thereby considered that another effect dominated the plasmon nanofocusing process, which is the interaction between plasmons propagating at the silver–air interface and at the silver–oxidized silicon interface. The silver tapered structure has two surfaces, one of which is attached to the pyramidal oxidized silicon tip and the other is facing the air on the opposite side. Plasmons propagate on both sides after plasmon excitation at the grating structure. If the thickness of the silver tapered structure is larger than a certain value, plasmons on both sides propagate independently. However, when the silver thickness is smaller than that value, plasmons propagating on each side couple with each other, which creates two discrete propagation modes known as the long-range surface plasmon (LRSP) mode and the short-range surface plasmon (SRSP) mode. The LRSP mode is literally the mode that a plasmon can propagate for a long distance with very small energy loss during plasmon propagation. It is useful to send plasmon energy for a long distance; however, it is known that this mode is cut-off and does not contribute to the nanofocusing process.[24,25] Therefore, we cannot take the benefit of lower energy loss of plasmon propagation for plasmon nanofocusing. In contrast, the SRSP mode has a much shorter propagation length. Even though this mode actually contributes to the nanofocusing process, large propagation energy loss does not facilitate efficient plasmon nanofocusing, resulting in weak near-field intensity. We believe that this plasmon interaction has dominated the plasmon nanofocusing process for thicknesses smaller than 50 nm. The plasmon interaction occurs if the thickness becomes thinner than a few tens of nanometers,[26] and the effect becomes stronger as the thickness further decreases. This effect was significant especially in the cases where the silver thickness was smaller than 20 nm as one can see that no near-field light was excited at the apex.

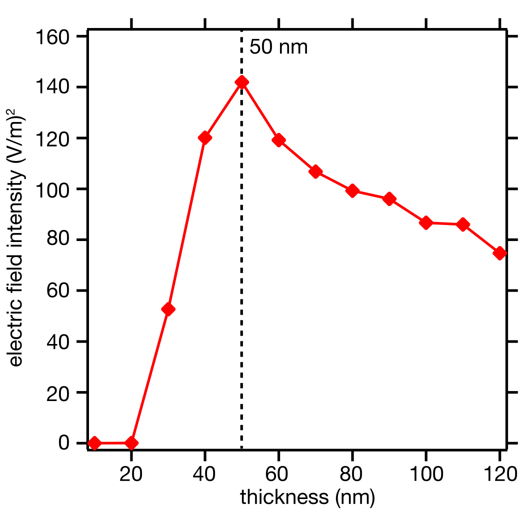

FIG. 3. Dependence of near-field light intensity on thickness of the silver tapered structure.

At last, we also investigated the cone angle. In our tip design, the cone angle was 28°, which was determined by the original base structure of the cantilever tip (NT-MDT, CSG01). In addition, there are several types of cantilevers available that have different cone angles. It is also possible to adjust the cone angle by nanolithographic techniques such as FIB milling. In this study, we varied the cone angle from 10° to 60°. The thickness and the grating period were set to 40 and 430 nm, respectively. Please note that a narrower cone angle leads to a shorter width of the grating coupler. When the width of the grating coupler becomes smaller than the incident focal size, this would affect the near-field light intensity because some parts of the incident light will be out of the grating area and will not hit the grating structure. This would mean that a reduced amount of plasmons will be excited at the grating in this case since the effective grating area illuminated with the incident light would be smaller. Therefore, for a meaningful comparison of the efficiency of plasmon nanofocusing, we have normalized the near-field intensity by the area of the grating structure when the width of the grating coupler is narrower than the incident focal size. Figure 4(a) shows the near-field intensity dependence on the cone angle. The near-field intensity increased with narrowing of the cone angle. A possible reason for the cone angle dependence is that at small cone angles, scattering loss (non-Ohmic loss) due to the sharp edges of the tapered structure is less than large cone angles, as previously reported that a narrow cone angle leads to a large degree of adiabaticity.[27] Therefore, we concluded that smaller cone angles are better for better efficiency of the plasmon nanofocusing process in our tip design.

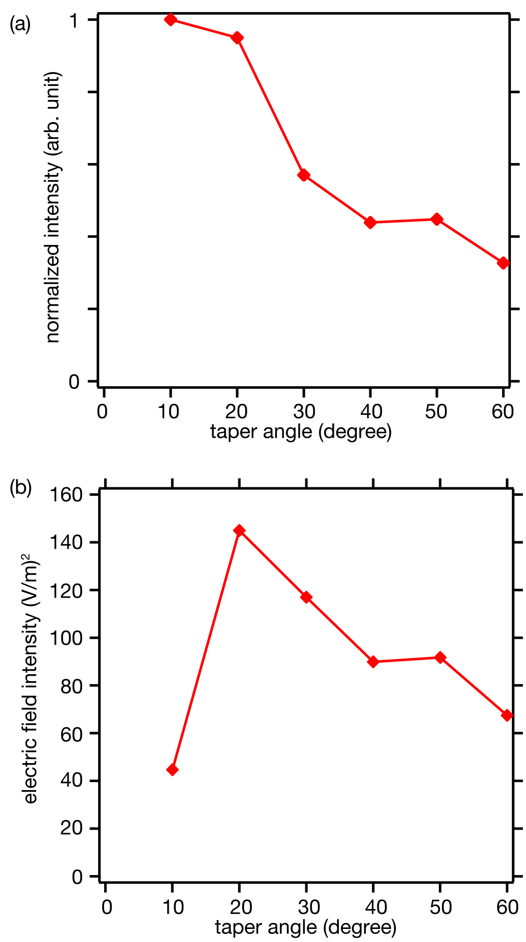

FIG. 4. (a) Dependence of near-field light intensity on the cone angle, normalized by the area of the grating structure. (b) Dependence of near-field light intensity on the cone angle without normalization.

We have also evaluated the dependence of near-field light intensity on the cone angle without normalizing it by the grating area because our interest is how much the near-field light intensity is practically obtained in the actual experimental situation. Although it is necessary to normalize the near-field intensity by the grating area to evaluate the efficiency of plasmon nanofocusing itself, one can understand the actual situation more reliably by including the excitation efficiency of plasmons at the grating structure, no matter how wide the grating structures are. Figure 4(b) shows the relationship between the near-field light intensity and the cone angle. We found that the strongest near-field light is obtained at a cone angle of 20°. The intensity was around 145.0 $(V/m)^2$. At angles larger than 20°, the near-field intensity gradually decreased to around 67.5 $(V/m)^2$. We guess that the reason is the same as mentioned above. The scattering loss at tapered edges during plasmon propagation increased at large cone angles. Much weaker near-field light was also obtained at a cone angle of 10°, which was around 44.7 $(V/m)^2$, even though the plasmon nanofocusing process itself is supposed to be efficient. We believe that this is due to weak plasmon excitation at the grating since the grating width is narrower than the incident focal size. The width of the grating coupler for a cone angle of 10° was around 700 nm, whereas the incident focal size was around 1900 nm. This indicates that most of incident light did not hit the grating and was not involved in the coupling process. For cone angles of 20° and 30°, the grating widths were ∼1410 and 2150 nm, respectively. We believe, therefore, that these cases showed relatively higher near-field light intensities as they have a good balance between sufficient grating size and narrow cone angles. We concluded that 20°–30° are the best values for the cone angle for our particular tip design and the experimental setup that we considered in the simulation, whereas narrower cone angles could be better for efficient plasmon nanofocusing.

III. CONCLUSION

In conclusion, we have numerically investigated the optical properties of near-field light generated on silver tapered structures made on pyramidal cantilever tips for plasmon nanofocusing. This particular tip design, which is practically easy to fabricate, holds great potential for future practical applications of plasmon-nanofocusing based NSOM owing to its various advantages and unique optical properties, which could be governed by the structural parameters of metallic tapered structure and cantilever tips used as a base. We observed a strong impact of the base material of the cantilever on the optical properties of the near-field light. By oxidizing a silicon cantilever tip, the near-field light intensity was significantly enhanced, which was around 120 $(V/m)^2$. The electric field intensity enhancement was further improved, to around 140 $(V/m)^2$, by further modifying the silver tapered structure on the oxidized silicon tip. On the other hand, the spatial confinement of near-field light at the tip apex was better in the case of silicon. From the practical viewpoint, we have made several important discussions on the cantilever material. Moreover, the thickness and the cone angle of the silver tapered structure are thoroughly investigated for this particular design. We conclude that with respect to the near-field light intensity, a thickness of ∼50 nm and a cone angle of ∼20° showed the highest intensity. In this study, we fixed the wavelength of incident light to 642 nm in order to focus our investigation on in-depth analysis of the structural parameters. However, the effect of these parameters would be different at different wavelengths, which we would like to leave for future work. In this research, we examined our unique tip design properties on structural parameters for plasmon nanofocusing. Considering the importance and practicability of this tip design that we developed, this research provides fundamental as well as practical insights to utilize it for near-field optical measurements and contributes toward further developments of plasmon-nanofocusing based NSOM and the related nanophotonic applications.

ACKNOWLEDGMENTS

This research was supported, in part, by the JSPS Core-to-Core program, the JSPS Grant-in-Aid for Scientific Research (A), Grant No. 19H00870, and the JSPS Grant-in-Aid for Scientific Research (B), Grant No. 20H02658. R.Y. would like to acknowledge the financial support from the JICA.

AUTHOR DECLARATIONS

Conflict of Interest

The authors have no conflicts to disclose.

Author Contributions

Ravi Yadav: Data curation (equal); Formal analysis (equal); Investigation (equal); Methodology (equal); Software (equal); Writing – original draft (equal). **Takayuki Umakoshi**: Funding acquisition (equal); Project administration (equal); Resources (equal); Supervision (equal); Writing – review & editing (equal). **Prabhat Verma**: Conceptualization (equal); Funding acquisition (equal); Project administration (equal); Resources (equal); Supervision (equal); Writing – review & editing (equal).

DATA AVAILABILITY

The data that support the findings of this study are available from the corresponding author upon reasonable request.

REFERENCES

[1] N. Kumar, B. M. Weckhuysen, A. J. Wain, and A. J. Pollard, "Nanoscale chemical imaging using tip-enhanced Raman spectroscopy," Nat. Protoc. **14**(4), 1169–1193 (2019).

[2] I. Maouli, A. Taguchi, Y. Saito, S. Kawata, and P. Verma, "Optical antennas for tunable enhancement in tip-enhanced Raman spectroscopy imaging," Appl. Phys. Express **8**(3), 032401-1–032401-3 (2015).

[3] P. Verma, T. Ichimura, T. Yano, Y. Saito, and S. Kawata, "Nano-imaging through tip-enhanced Raman spectroscopy: Stepping beyond the classical limits," Laser Photonics Rev. **4**(4), 548–561 (2010).

[4] T. Umakoshi, Y. Saito, and P. Verma, "Fabrication of near-field plasmonic tip by photoreduction for strong enhancement in tip-enhanced Raman spectroscopy," Appl. Phys. Express **5**(5), 052001-1–052001-3 (2012).

[5] T.-a. Yano, P. Verma, Y. Saito, T. Ichimura, and S. Kawata, "Pressure-assisted tip-enhanced Raman imaging at a resolution of a few nanometres," Nat. Photonics **3**(8), 473–477 (2009).

[6] P. Verma, "Tip-enhanced Raman spectroscopy: Technique and recent advances," Chem. Rev. **117**(9), 6447–6466 (2017).

[7] R. Kato, T. Umakoshi, R. T. Sam, and P. Verma, "Probing nanoscale defects and wrinkles in MoS_2 by tip-enhanced Raman spectroscopic imaging," Appl. Phys. Lett. **114**(7), 073105-1–073105-5 (2019).

[8] S. Kawata, Y. Inouye, and P. Verma, "Plasmonics for near-field nano-imaging and superlensing," Nat. Photonics **3**, 388–394 (2009).

[9] K. V. Nerkararyan, "Superfocusing of a surface polariton in a wedge-like structure," Phys. Lett. A **237**(1–2), 103–105 (1997).

[10] M. I. Stockman, "Nanofocusing of optical energy in tapered plasmonic waveguides," Phys. Rev. Lett. **93**(13), 137404-1–137404-4 (2004).

[11] D. K. Gramotnev, M. W. Vogel, and M. I. Stockman, "Optimized nonadiabatic nanofocusing of plasmons by tapered metal rods," J. Appl. Phys. **104**(3), 034311-1–034311-8 (2008).

[12] S. Berweger, J. M. Atkin, R. L. Olmon, and M. B. Raschke, "Adiabatic tip-plasmon focusing for nano-Raman spectroscopy," J. Phys. Chem. Lett. **1**(24), 3427–3432 (2010).

[13] C. Ropers, C. C. Neacsu, T. Elsaesser, M. Albrecht, M. B. Raschke, and C. Lienau, "Grating-coupling of surface plasmons onto metallic tips: A nanoconfined light source," Nano Lett. **7**(9), 2784–2788 (2007).

[14] S. Kim, N. Yu, X. Ma, Y. Zhu, Q. Liu, M. Liu, and R. Yan, "High external-efficiency nanofocusing for lens-free near-field optical nanoscopy," Nat. Photonics **13**(9), 636–643 (2019).

[15] T. Umakoshi, M. Tanaka, Y. Saito, and P. Verma, "White nanolight source for optical nanoimaging," Sci. Adv. **6**(23), eaba4179 (2020).

[16] V. Kravtsov, R. Ulbricht, J. M. Atkin, and M. B. Raschke, "Plasmonic nanofocused four-wave mixing for femtosecond near-field imaging," Nat. Nanotechnol. **11**, 459–464 (2016).

[17] T. Umakoshi, Y. Saito, and P. Verma, "Highly efficient plasmonic tip design for plasmon nanofocusing in near-field optical microscopy," Nanoscale **8**(10), 5634–5640 (2016).

[18] R. Yadav, H. Arata, T. Umakoshi, and P. Verma, "Plasmon nanofocusing for the suppression of photodegradation in fluorescence imaging using near-field scanning optical microscopy," Opt. Commun. **497**, 127206 (2021).

[19] K. Taguchi, T. Umakoshi, S. Inoue, and P. Verma, "Broadband plasmon nanofocusing: Comprehensive study of broadband nanoscale light source," J. Phys. Chem. C **125**, 6378–6386 (2021).

[20] P. B. Johnson and R. W. Christy, "Optical constants of the noble metals," Phys. Rev. B **6**(12), 4370–4379 (1972).

[21] D. E. Aspnes and A. A. Studna, "Dielectric functions and optical parameters of Si, Ge, GaP, GaAs, GaSb, InP, InAs, and InSb from 1.5 to 6.0 eV," Phys. Rev. B **27**(2), 985–1009 (1983).

[22] K. Luke, Y. Okawachi, M. R. E. Lamont, A. L. Gaeta, and M. Lipson, "Broadband mid-infrared frequency comb generation in a Si_3N_4 microresonator," Opt. Lett. **40**(21), 4823–4826 (2015).

[23] I. H. Malitson, "Interspecimen comparison of the refractive index of fused silica," J. Opt. Soc. Am. **55**(10), 1205–1209 (1965).

[24] F. De Angelis, R. P. Zaccaria, M. Francardi, C. Liberale, and E. Di Fabrizio, "Multi-scheme approach for efficient surface plasmon polariton generation in metallic conical tips on AFM-based cantilevers," Opt. Express **19**(22), 22268–22279 (2011).

[25] R. P. Zaccaria, F. De Angelis, A. Toma, L. Razzari, A. Alabastri, G. Das, C. Liberale, and E. Di Fabrizio, "Surface plasmon polariton compression through radially and linearly polarized source," Opt. Lett. **37**(4), 545–547 (2012).

[26] J. Takahara and M. Miyata, "Mutual mode control of short- and long-range surface plasmons," Opt. Express **21**(22), 27402–27410 (2013).

[27] C. C. Neacsu, S. Berweger, R. L. Olmon, L. V. Saraf, C. Ropers, and M. B. Raschke, "Near-field localization in plasmonic super-focusing: A nanoemitter on a tip," Nano Lett. **10**, 592–596 (2010).